Efficient mRNA delivery using lipid nanoparticles modified with fusogenic coiled-coil peptides

Zeng, Y.; Shen, M.; Pattipeiluhu, R.; Zhou, X.; ZHANG, Y.; Bakkum, T.; ... ; Kros, A.

Nanoscale

PAPER

Check for updates

Efficient mRNA delivery using lipid nanoparticles modified with fusogenic coiled-coil peptides†

Ye Zeng,[a] Mengjie Shen,[a] Roy Pattipeiluhu,[a] Xuequan Zhou,[a] Yun Zhang,[a] Thomas Bakkum,[a] Thomas H. Sharp,[b] Aimee L. Boyle [ID][a] and Alexander Kros [ID] *[a]

Gene delivery has great potential in modulating protein expression in specific cells to treat diseases. Such therapeutic gene delivery demands sufficient cellular internalization and endosomal escape. Of various nonviral nucleic acid delivery systems, lipid nanoparticles (LNPs) are the most advanced, but still, are very inefficient as the majority are unable to escape from endosomes/lysosomes. Here, we develop a highly efficient gene delivery system using fusogenic coiled-coil peptides. We modified LNPs, carrying EGFP-mRNA, and cells with complementary coiled-coil lipopeptides. Coiled-coil formation between these lipo-peptides induced fast nucleic acid uptake and enhanced GFP expression. The cellular uptake of coiled-coil modified LNPs is likely driven by membrane fusion thereby omitting typical endocytosis pathways. This direct cytosolic delivery circumvents the problems commonly observed with the limited endosomal escape of mRNA. Therefore fusogenic coiled-coil peptide modification of existing LNP formulations to enhance nucleic acid delivery efficiency could be beneficial for several gene therapy applications.

Introduction

An understanding of both the human genome and disease mechanisms has expanded our knowledge of gene-dysregulation related diseases, paving the way for novel gene therapies.[1–3] Gene therapy potentially enables the treatment of disease at the genetic level by correcting or replacing malfunctioning genes.[4] This repair or replacement could be achieved by delivering exogenous nucleic acids such as DNA, mRNA, small interfering RNA (siRNA), microRNA (miRNA), or antisense oligonucleotides (ASO) to the tissue or organ of interest.[2] However, the complexity of cell membranes and cellular barriers impedes the efficient transfer of the genetic cargo into the organs, tissue, and cells of interest, resulting in a poor therapeutic effect.[4,5]

Since nucleic acid-based drugs are unable to enter cells and are inherently unstable *in vivo*, a drug delivery system is required. An ideal gene vector should transfect the desired tissue or organ efficiently, while the vector should be non-toxic, non-immunogenic, and easy to formulate. State-of-the-art gene vectors are divided into two major classes: viral and nonviral. As viral vectors typically possess high cellular transduction efficiency, many gene therapy clinical trials are using modified viral vectors such as lentiviruses, retroviruses, adenoviruses, and adenovirus-associated viruses.[4,6–8] However, the widespread use of viral vectors is hampered because of side-effects including potential carcinogenesis, immunogenicity, broad tropism, limited DNA packaging capacity, and difficulty of vector production.[2,9,10] In contrast, nonviral vectors could potentially circumvent these limitations, especially in terms of safety and the size of encapsulated genetic cargo.[11] Nonviral gene vectors in (pre)clinical applications are commonly composed of lipids,[12] lipoids,[13] or are polymer-based.[2]

Currently, the most advanced nonviral nucleic acid delivery system is lipid nanoparticles (LNPs).[14–16] LNPs are composed of an ionizable lipid to condense the genetic cargo and release it after entering the cells; a cholesterol moiety to stabilize the LNP structure; a helper lipid; and a PEGylated lipid to improve colloidal stability and reduce protein absorption.[17] The first siRNA drug, named Onpattro (Patisiran), was approved in 2018 by the FDA and was designed to treat polyneuropathies induced by hereditary transthyretin-mediated amyloidosis (hATTR) in adults. This therapy has been a milestone for non-viral nucleic acid-based therapies.[1] Onpattro is a lipid nanoparticle (LNP) formulation that upon intravenous administration binds serum apolipoprotein E (ApoE), which acts as an endogenous targeting ligand to the low-density lipoprotein receptor present in hepatocytes.[18]

LNPs cell entry relies on endocytosis, and the efficacy is dependent on the delivery of encapsulated siRNA to the

[a]Department of Supramolecular & Biomaterials Chemistry, Leiden Institute of Chemistry, Leiden University, Einsteinweg 55, 2333 CC Leiden, The Netherlands. E-mail: a.kros@chem.leidenuniv.nl
[b]Department of Cell and Chemical Biology, Section Electron Microscopy, Leiden University Medical Center, 2300 RC Leiden, The Netherlands
†Electronic supplementary information (ESI) available. See DOI: https://doi.org/10.1039/d3nr02175k
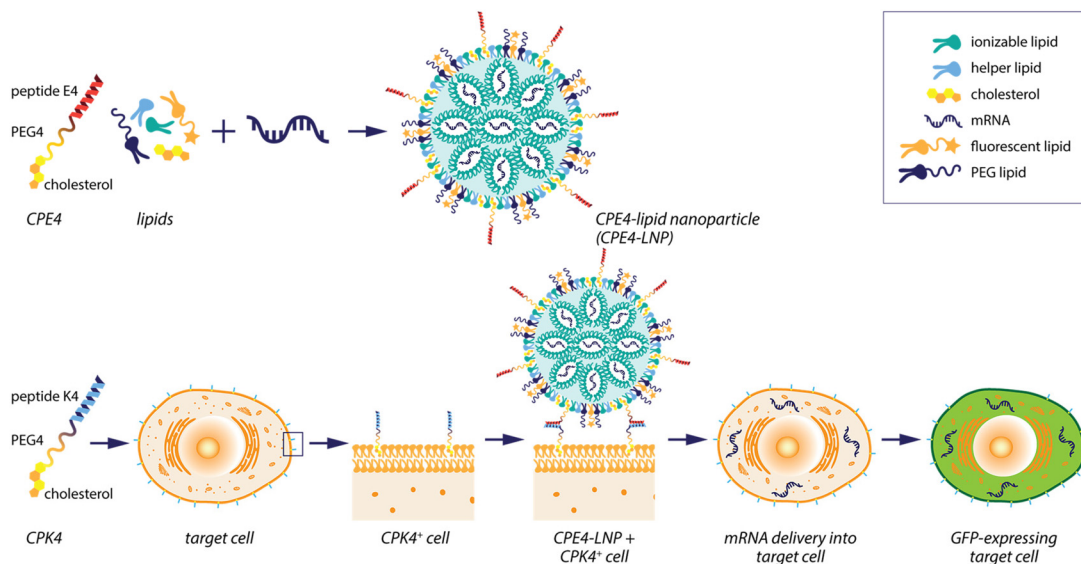
Scheme 1 Schematic representation of the nonviral lipid nanoparticles (LNPs) that induce efficient mRNA delivery within cells when modified with fusogenic coiled-coil peptides.

cytoplasm.[15] However, LNPs (and other nanoparticles) transport the encapsulated macromolecules to different subcellular destinations, the majority of which accumulate in lysosomes for degradation.[19] Studies showed only <2% of the siRNA in LNPs was able to escape endosomal compartments, resulting in the release into the cytoplasm;[20] and <5% of cytoplasmic mRNA of LNPs was distributed outside of endosomes, corresponding to endosome escaped events.[21] Therefore, there is an urgent need to overcome this major limitation of inefficient nucleic acid delivery into cells. Many attempts have been reported to facilitate endosomal escape by using polyplex-mediated endosomal swelling nanomaterials,[22,23] cell-penetrating peptides (CPPs),[24,25] or exogenous stimuli-responsive biomaterials responding to specific biochemical conditions, such as change in pH or redox state but to date, there is still a lack of modified systems resulting in efficient endosomal escape.[22,26]

One way that cells transfer components is *via* membrane fusion. Therefore, membrane fusion is critical for many biological processes, including organelle inheritance in cell growth and division, chemical synaptic transmission in the nervous system, and the modulation of synaptic strength in memory and learning.[27] The docking of transport vesicles to the target plasma membrane in neuronal exocytosis is triggered by coiled-coil formation between complementary SNARE protein subunits.[28] Inspired by the SNARE protein complex, our group has developed a synthetic membrane fusion system based on a heterodimeric coiled-coil peptide pair and we have demonstrated direct drug delivery into the cytosol of living cells *in vitro* and *in vivo*.[29–32]

In this study, we applied our fusogenic coiled-coil peptides to efficiently deliver LNPs into cells to enhance genetic cargo transfection efficacy *via* membrane fusion. We developed

coiled-coil peptide modified LNPs encapsulating EGFP-mRNA to induce efficient cellular delivery and concomitant GFP expression (Scheme 1). The LNP formulation was modified with lipopeptide CPE4 (CPE4-LNP) while cells were pretreated with the complementary lipopeptide CPK4. The addition of CPE4-LNP to the cells resulted in efficient LNP uptake and protein expression, which was observed and studied by confocal microscopy and flow cytometry. By applying different endocytosis inhibitors and a lysosome tracker, the internalization pathway was investigated. This study demonstrates that, by utilizing coiled-coil peptides, significant amounts of genetic cargo can be delivered to cells by evading endocytosis pathways.

Results and discussion

Comparison of K3/E3 and K4/E4 coiled-coil interactions

Our previous studies showed that both the K3/E3 and K4/E4 coiled-coil pairs (where 3 and 4 correspond to the number of heptad repeats within the peptides), induced efficient and targeted membrane fusion between liposomes, and liposomes with cells, both *in vitro* and *in vivo*.[29–32] In order to determine which pair was most suitable for this study we evaluated their coiled-coil forming and cargo delivery properties. Circular dichroism (CD) spectroscopy (Fig. S1a†), confirmed both K3/E3 and K4/E4 pairs formed coiled coils efficiently. The K4/E4 pair is composed of one additional heptad repeat compared to K3/E3, and as expected the former peptide pair yielded a more-folded complex. Cellular internalization of En-modified fluorescent liposomes in Kn-modified HeLa cells was subsequently quantified by flow cytometry (Fig. S1b†), demonstrating that both K3/E3 and K4/E4 induced cellular uptake,

however K4/E4 exhibited significantly higher cell uptake. When comparing the mean fluorescence intensity (MFI) of fluorescent cells (Fig. S1c and d†), we observed that the K4/E4 pair is the most fusogenic as the cells showed the highest levels of fluorescence. We also observed that CPK4 modified liposomes were able to enter cells quite efficiently when the cells were pretreated with CPE4 and even in the absence of CPE4, presumably due to non-specific electrostatic interactions between the positively charged CPK4 lipopeptides and the negatively charged cell membranes. To exclude that undesirable electrostatic interaction, we decided to focus on the E modified lipid-nanoparticles, while cells pretreated with CPK.

Next, we studied whether these findings were also valid for the delivery of LNPs to cells. We formulated LNPs encapsulating Alexa488-labeled nucleic acid and modified these with 1 mol% of either CPE3 or CPE4 yielding CPE3-LNP and CPE4-LNP. HeLa cells were pretreated with the complementary CPKn and cellular uptake of the LNPs was quantified by flow cytometry measurements. Again, the CPK4/CPE4 pair exhibited enhanced cellular uptake as compared to the CPK3/CPE3 pair (Fig. S1e and f†).

Therefore, we utilized the K4/E4 peptide pair with CPK4 at the cell membrane and CPE4 in the LNPs in the following experiments to achieve optimal coiled-coil formation.

Lipid nanoparticle characterization

The lipid composition of the clinically approved LNP formulation Onpattro (Dlin-MC3-DMA : cholesterol : DSPC : DMG-PEG2K = 50 : 38.5 : 10 : 1.5) has been optimized for potent silencing of protein expression in cells by delivery of siRNA.[1] To investigate the efficacy of coiled-coil mediated mRNA delivery into cells, we opted to formulate CPE4-LNP with the same lipid composition as Onpattro and added 1 mol% of CPE4 (Fig. 1a and b). Dynamic light scattering (DLS) was used to determine the hydrodynamic diameters of both plain and CPE4-modified LNPs after encapsulating EGFP-mRNA. These diameters were found to be 80 and 95 nm respectively with low polydispersities (PDI) (Fig. 1c). Both formulations had a near-neutral zeta-potential, thus the presence of 1 mol% CPE4 did not influence the surface charge significantly. mRNA encapsulation efficiency was slightly lower for CPE4-LNP, which might be due to electrostatic repulsion between the negatively charged peptide E and the mRNA. Nonetheless, the encapsulation efficiency exceeded 85%. Cryogenic transmission electron microscopy (cryo-EM) imaging revealed a spherical morphology for CPE4-LNP, similar to plain LNP, and the majority of both LNPs (>80%) had a diameter of 30–70 nm (Fig. 1d and e). The long-term colloidal stability of both LNPs was determined for 10 days and no discernable deviations were observed in either diameter or PDI, indicating that both LNP formulations were stable over this timeframe (Fig. 1f). Upon replacing EGFP-mRNA with Alexa488 labeled nucleic acid, the size distribution and morphology were identical to the EGFP-mRNA encapsulated LNPs (Fig. S2a–c†). In summary, the addition of 1 mol% of coiled-coil peptide CPE4 to plain LNP did not change the physicochemical properties of LNPs, thus differences in cell uptake and protein expression can be related to the presence of coiled-coils (*vide infra*).
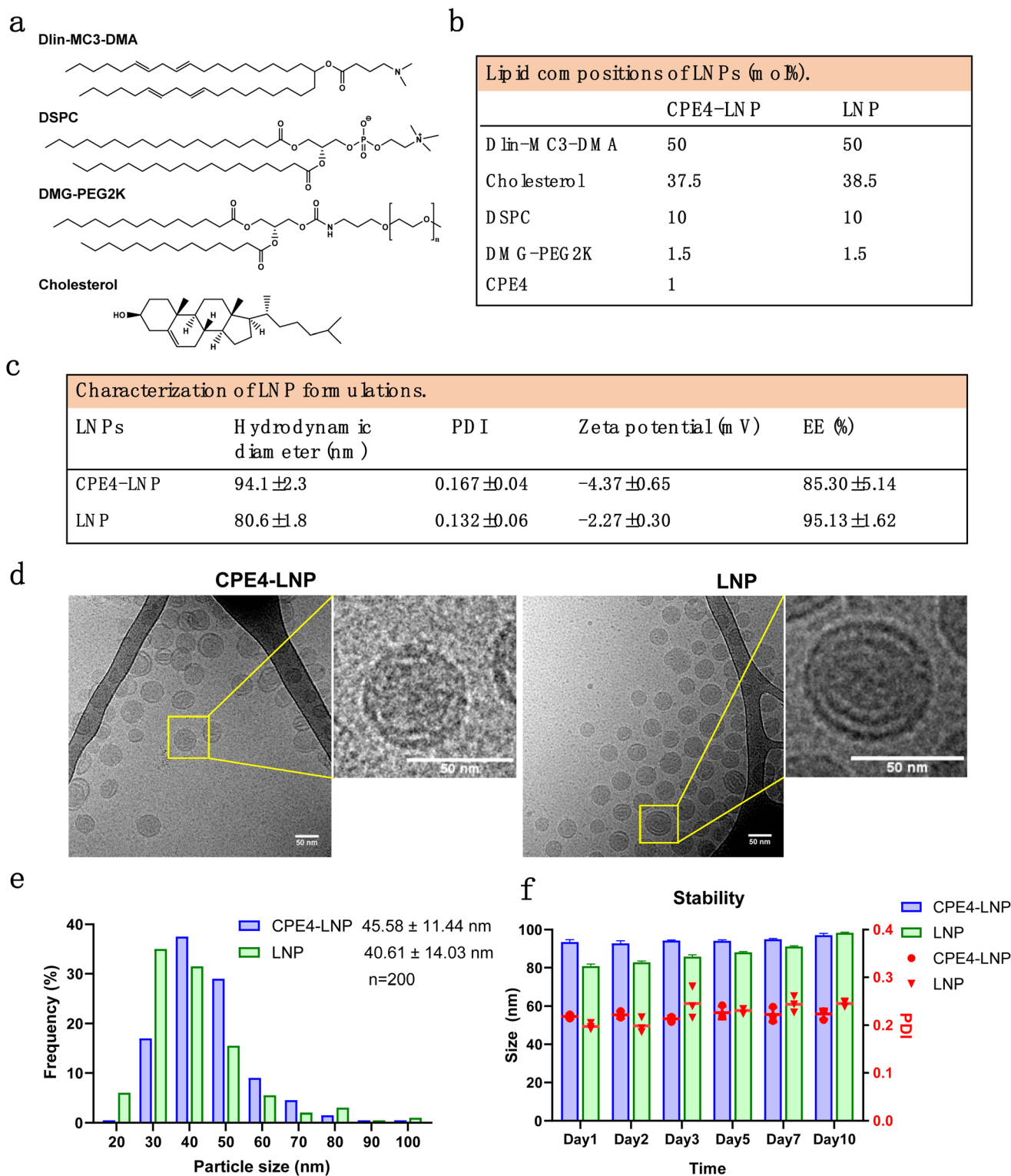
Cell uptake of LNPs

The uptake of LNPs containing Alexa-488 nucleic acid in HeLa cells and the influence of the E4/K4 coiled-coil pair was studied using confocal microscopy and flow cytometry measurements for qualitative and quantitative analysis (Fig. S3a†). The plain LNP formulation served as a control, and 1 mol% of red-fluorescent PE-LR was added to follow the uptake and location of the lipids. Confocal microscopy imaging revealed that CPK4 decorated HeLa cells induced abundant Alexa488-labeled nucleic acid cellular uptake after only 15 minutes of incubation with CPE4-LNP (Fig. 2a). If LNPs enter cells *via* a process of membrane fusion, it is expected that the lipid dye PE-LR remains mainly bound to the plasma membrane while the content (*i.e.* nucleic acid) enters the cytoplasm.[33,34] Interestingly, colocalization of Alexa488 nucleic acid and PE-LR decreased, indicating that membrane fusion and content nucleic acid release indeed had occurred when using the coiled-coil peptides CPE4/CPK4. In contrast, in plain LNP or control experiments in which only one of the coiled-coil peptides was present, only limited nucleic acid and lipid uptake could be detected.

Flow cytometry was used to quantify the cellular uptake of the LNPs. The most efficient uptake was observed when HeLa cells were pretreated with CPK4 and incubated with CPE4-LNP, in accordance with the confocal microscopy study. Within 15 minutes of incubation, 99.9% of the cells had nucleic acid internalized, while plain LNP or the control groups revealed negligible delivery (Fig. 2b). In addition, the mean fluorescence intensity (MFI) analysis of the Alexa488-nucleic acid internalized by cells was significantly higher when coiled-coil peptides were used over all other groups (Fig. 2c and d). These results confirmed that the fusogenic coiled-coil system induced rapid and efficient nucleic acid cellular uptake.

To study whether the E4/K4 pair is able to enhance nucleic acid delivery in other cell types, Chinese hamster ovary (CHO), mouse fibroblast NIH/3T3, and human T cell lymphocyte Jurkat cells were transfected with LNPs. Again, CPK4-pretreated cells incubated with CPE4-LNP for 15 minutes resulted in the highest uptake of nucleic acid, regardless of cell type (Fig. 3a, Fig. S3b and c†). In line with previous results on HeLa cells, negligible nucleic acid delivery was observed for plain LNP and all control groups with CHO and NIH/3T3 cells, consistent with flow cytometry analysis (Fig. 3b and c). Jurkat cells are regarded as a hard-to-transfect cell line.[35–38] By applying our fusogenic coiled-coil peptides, CPK4-pretreated Jurkat cells incubated with CPE4-LNP produced superior nucleic acid internalization (Fig. 3a–c and Fig. S3d†), as compared to all other groups, which showed only limited nucleic acid uptake.

Altogether, this cell uptake study confirmed that fusogenic coiled-coil modified LNP can efficiently deliver nucleic acid in high yields to various cell lines as compared to the clinically approved LNP formulation.

a

Dlin-MC3-DMA

DSPC

DMG-PEG2K

Cholesterol

b

Lipid compositions of LNPs (mol%).		
	CPE4-LNP	LNP
Dlin-MC3-DMA	50	50
Cholesterol	37.5	38.5
DSPC	10	10
DMG-PEG2K	1.5	1.5
CPE4	1	

c

Characterization of LNP formulations.				
LNPs	Hydrodynamic diameter (nm)	PDI	Zeta potential (mV)	EE (%)
CPE4-LNP	94.1 ± 2.3	0.167 ± 0.04	−4.37 ± 0.65	85.30 ± 5.14
LNP	80.6 ± 1.8	0.132 ± 0.06	−2.27 ± 0.30	95.13 ± 1.62

d

CPE4-LNP   LNP

e

CPE4-LNP 45.58 ± 11.44 nm
LNP 40.61 ± 14.03 nm
n=200

f

Stability

Fig. 1 Design and characterization of LNPs carrying EGFP-mRNA. (a) Structures of lipids used for the preparation of LNPs. (b) Lipid composition of LNPs (mol%). (c) Characterization of LNPs. (d) Cryo-EM images of LNPs. The scale bar is 50 nm. (e) Size distribution of EGFP-mRNA encapsulated LNPs as determined by cryo-EM. The values were calculated from the size distribution frequency. (f) Long-term stability of LNPs. LNPs were stored at 4 °C in a PBS buffer. The nanoparticle diameter and PDI were monitored by DLS (mean ± s.d., n = 3).
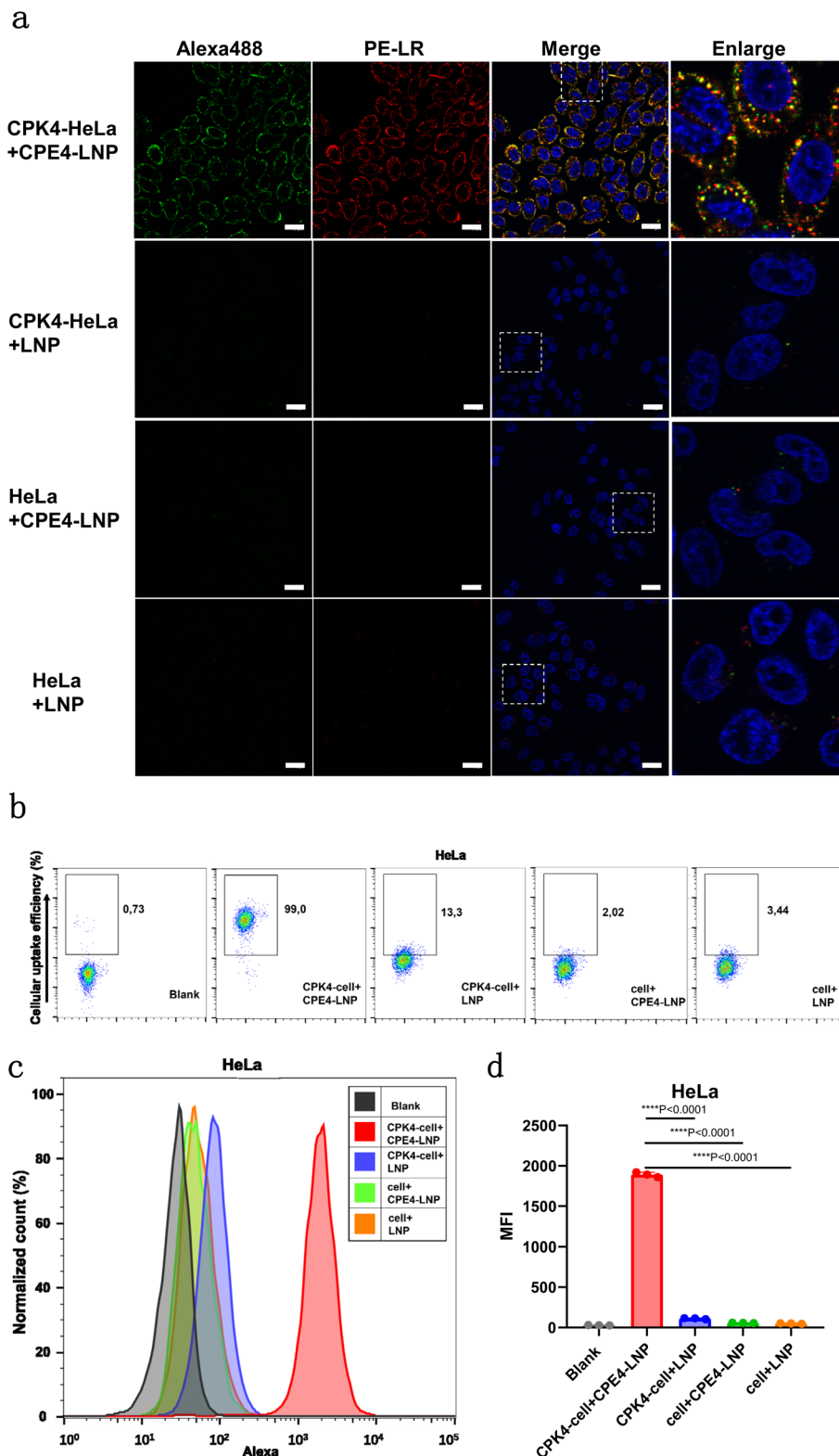
Fig. 2 Nucleic acid delivery to HeLa cells using fusogenic coiled-coil LNPs. (a) Confocal microscopy images of cellular internalization of LNPs with HeLa cells. HeLa cells were pretreated with micellar CPK4 (10 μM, 200 μL) for 2 hours. After removal of the supernatant, cells were incubated with CPE4-LNP containing Alexa488-nucleic acid (200 μM, 200 μL) for 15 minutes, washed, and imaged. Blue: Hoechst 33342; green: Alexa488-nucleic acid; red: LR-PE; BF: bright field. The scale bar is 20 μm. (b) Cellular internalization efficiency of LNPs with HeLa cells quantified by flow cytometry (representative dataset from $n = 3$ per group). (c and d) Fluorescence intensity of cells treated with LNPs carrying Alexa488-nucleic acid. An unpaired student t-test was used to determine the significance of the comparisons of data indicated in d ($*P < 0.05$; $**P < 0.01$; $***P < 0.001$; $****P < 0.0001$). In all panels, error bars represent the mean $\pm$ s.d. (representative dataset from $n = 3$ biologically independent samples).
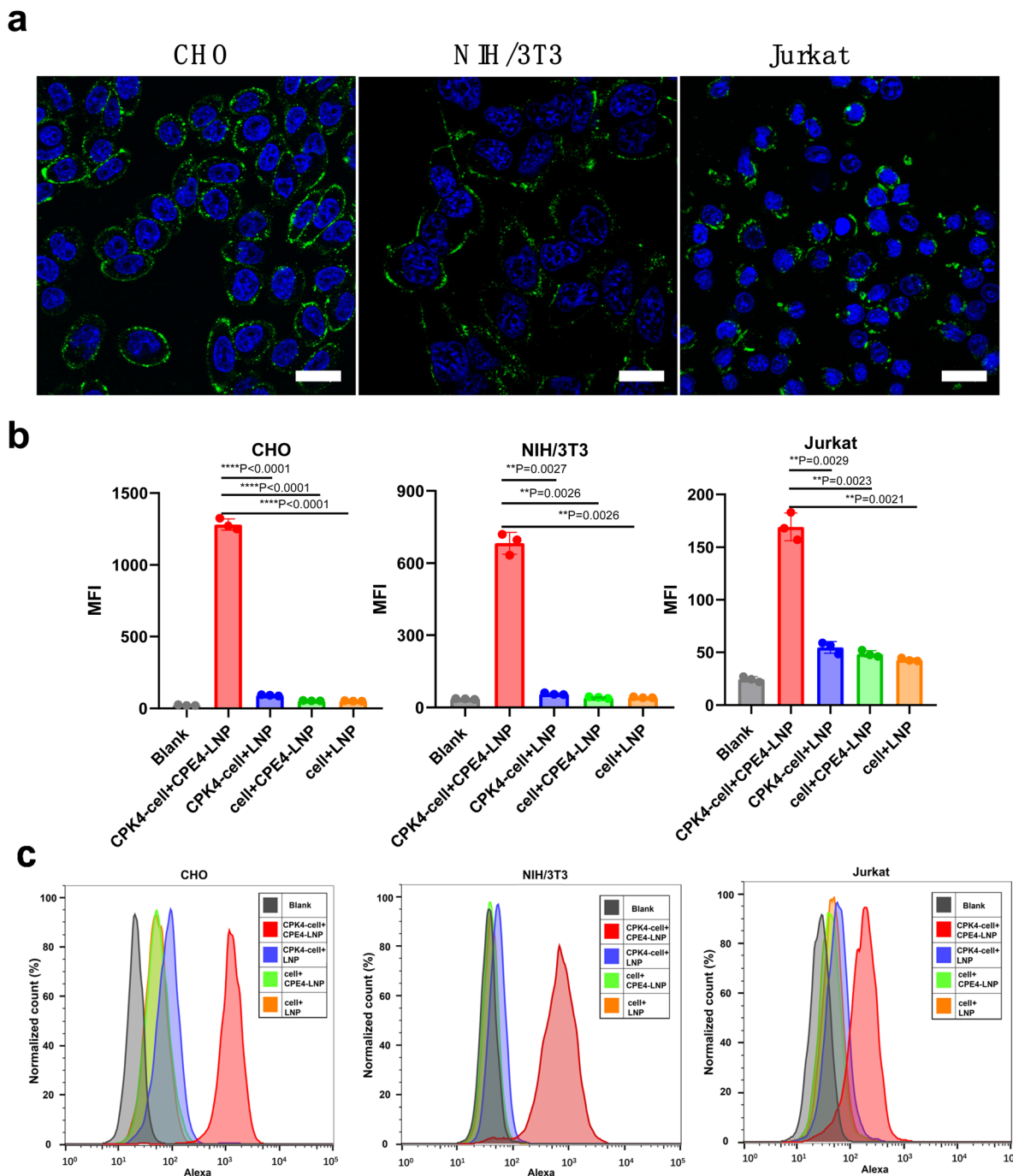
Fig. 3 Evaluation of cellular nucleic acid delivery by coiled-coil functionalized LNPs with other cell lines. (a) Confocal images of CPE4-LNP with CPK4 pretreated CHO, NIH/3T3, and Jurkat cells. Blue: Hoechst 33342; green: Alexa488-nucleic acid. Scale bar is 20 μm. (b and c) The fluorescence intensity of internalized LNPs in CHO, NIH/3T3, and Jurkat cells. Alexa488-nucleic acid served as the fluorescent dye. Cells were pretreated with a micellar CPK4 solution (10 μM, 200 μL, 2 h), and after removal of the medium LNPs containing Alexa488-nucleic acid were added (200 μM, 200 μL, 15 min), and the cells were washed again before confocal and flow cytometry measurements (representative dataset from $n = 3$ per group). Unpaired student t-test was used to determine the significance of the comparisons of data indicated in b (*$P < 0.05$; **$P < 0.01$; ***$P < 0.001$; ****$P < 0.0001$). In all panels, error bars represent mean ± s.d. (representative dataset from $n = 3$ biologically independent samples).

Evaluation of lysosome co-localization

Effective nucleic acid internalization and subsequent transfection require efficient escape of the genetic cargo from endo-

somes/lysosomes into the cytosol.[39,40] However, this is typically an inefficient process, as most of the cargo is not released thus the therapeutic effect is lowered. Therefore novel approaches that facilitate direct cytosolic delivery, and bypass endosomal

entrapment, resulting in enhanced transfection efficiency are needed.

Coiled-coil mediated uptake of LNPs was studied as a function of time. For this, CPK4-pretreated cells were incubated with CPE4-LNPs encapsulating fluorescent nucleic acids for 15 minutes and colocalization analysis of nucleic acid with lysosome was studied. Confocal imaging revealed negligible nucleic acid colocalization with lysosomes during the following 0–8 h as confirmed by Pearson's correlation coefficient (PCC) and Mander's overlap coefficient (MOC) calculations, with the majority being dispersed in the cytosol (Fig. 4a and b). In contrast, Gilleron *et al.* quantified siRNA delivered to cells using LNPs and found that up to 70% was colocalized with lysosomes.[20]

Our data strongly suggests that fusogenic coiled-coil peptides enhance the cellular uptake of LNPs and increase the delivery of genetic cargo to the cytosol of cells, bypassing accumulation in endosomes and lysosomes. Therefore this approach holds promise for efficient transfection of cells with functional mRNA.

Cellular uptake mechanism of LNPs

As our fusogenic coiled-coil system appears to facilitate membrane fusion, we wanted to discover whether the uptake mechanism of coiled-coil peptide modified LNPs was different from plain LNPs. Therefore coiled-coil mediated cell uptake of LNPs was studied in the presence of different cellular endocytosis inhibitors (*i.e.* Wortmannin,[41,42] Nocodazole,[43] Pitstop 2,[44] Dynasore,[45,46] Genistein,[47,48] Methyl-β-cyclodextrin (MβCD),[47,49] and Sodium azide[50]).

Cellular uptake of nucleic acid in the presence of endocytosis inhibitors was analyzed by flow cytometry (Fig. 4c), and the fluorescence intensity was normalized against the non-inhibitor treated group (control: CPK4-HeLa + CPE4-LNP). None of the endocytosis inhibitors appeared to influence the cellular uptake of nucleic acid, although incubation at 4 °C seemed to decrease the uptake efficiency slightly. Confocal imaging also demonstrated that there were no apparent adverse effects on nucleic acid delivery as the overall distribution in the presence of all tested inhibitors was still comparable to the control group (Fig. S4a†). These results support the hypothesis that the dominant cell uptake pathway for coiled-coil mediated nucleic acid delivery is independent of typical endocytosis and is mainly membrane fusion mediated. This pathway avoids endosomal entrapment of genetic cargo and results in enhanced transfection.

For unmodified LNP, cell entry is dependent on endocytic pathways.[40,51] Gilleron *et al.* showed that dynasore reduced LNP uptake by around ~75%.[20] Hence, the cellular uptake mechanism of unmodified LNP was evaluated as a contrast to the fusogenic coiled-coil LNP system. To ensure sufficient cell uptake, plain LNP was incubated with cells for 4 hours. As expected, flow cytometry and confocal imaging of the cellular uptake of plain LNP showed nucleic acid internalization was remarkably reduced by NaN₃, dynasore, and incubation at 4 °C (Fig. 4d and Fig. S4b†). These results confirm that internaliz-

ation of unmodified LNP is mainly mediated by clathrin-dependent endocytosis.

In summary, while unmodified LNP uptake is mediated by the clathrin-dependent endocytic pathway, our fusogenic coiled-coil LNP system successfully delivered nucleic acid into cells through membrane fusion, avoiding endosomal entrapment of nucleic acid and resulting in enhanced nucleic acid delivery.

mRNA transfection

Gene therapy requires a high transfection efficiency to fulfill successful gene-modulating effects. We have shown that fusogenic coiled-coil peptides can improve the delivery of nucleic acids to the cytosol of cells. We then evaluated the transfection performance of the modified LNPs. For this, EGFP-mRNA was encapsulated in LNPs and after transfection, the expression of green fluorescent protein (GFP) was quantified as an easily detectable indicator for functional mRNA delivery. The mRNA concentrations of LNPs were determined by the RiboGreen RNA assay.

Four cell lines were used to study the gene transfection efficiency: HeLa, CHO, NIH/3T3, and Jurkat. Confocal imaging of transfected HeLa cells showed that CPK4-pretreated HeLa cells incubated with CPE4-LNP carrying EGFP-mRNA for 2 hours achieved the highest level of GFP expression, as almost every cell produced strong and uniform GFP expression (Fig. 5a). In contrast, the commonly used commercial transfection reagent lipofectamine 3000 (Lipo3K) only transfected a few cells. LNP and the control groups that lack one of the peptides achieved only minor GFP expression. Quantitative analysis by flow cytometry confirmed the confocal imaging study (Fig. 5b). The fusogenic coiled-coil mediated LNP delivery achieved almost quantitative GFP expression in all cells (99.9%), while lipofectamine 3000 mediated transfection resulted in 54.7% GFP positive cells. In addition, all other groups lacking either one or both peptides failed to induce relevant levels of GFP expression. Analysis of the GFP mean fluorescence intensity also illustrated that coiled-coil mediated delivery induced a 50-fold increase in GFP expression as compared to LNP and all other groups (Fig. 5c, d and Fig. S7a†). Interestingly, non-CPK4 pretreated HeLa cells incubated with CPE4-LNP induced a reasonable level of GFP-positive cells. However, the MFI in these GFP-positive cells was significantly lower as compared to the fusogenic coiled-coil group. The prolonged incubation time of the cells with CPE4-LNP in this experiment (2 hours) might be the cause for this observation.

Next, transfection of cells with EGFP-mRNA was investigated in other cell lines. CHO and NIH/3T3 cells also showed a robust GFP expression using the fusogenic coiled-coil peptides (Fig. S5a–d†). Again, the peptide-mediated delivery of mRNA was superior compared to plain LNP or the control groups lacking one of the peptides. Transfection enhancement by the fusogenic coiled-coil LNP system compared to plain LNP was >50-fold in HeLa cells, 63-fold in CHO cells, and 29-fold in NIH/3T3 cells (Fig. S7a–c†).
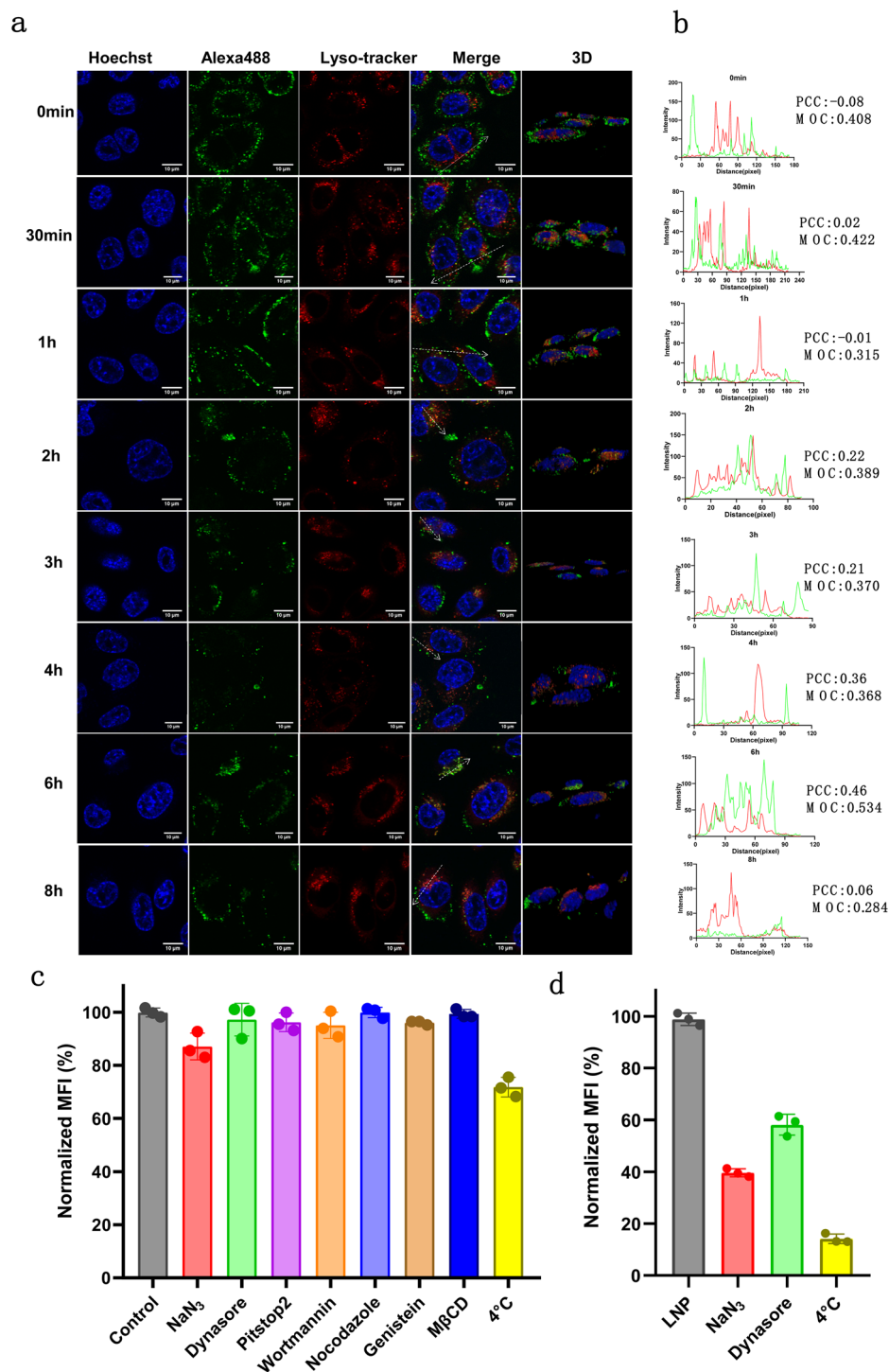
Fig. 4 Investigation of cellular delivery pathways of LNPs by fusogenic coiled-coil peptides. (a) Confocal images of coiled-coil mediated uptake of LNPs as a function of incubation time in HeLa cells after 15 min uptake; lysosome colocalization is studied by staining lysosomes with lyso-tracker deep red. HeLa cells were pretreated with CPK4 (10 μM, 200 μL) for 2 hours and incubated with CPE4-LNP carrying Alexa488-nucleic acid (200 μM, 200 μL) for 15 min, washed, and replaced by medium. Imaging was performed as a function of time. Blue: Hoechst 33342; green: Alexa488-nucleic acid; red: lyso-tracker deep red. The scale bar is 10 μm. (b) Quantitative colocalization analysis of Alexa488-nucleic acid (green curve) and lysosomes (red curve) in the dashed arrow area of the merge channel as a function of time using Image J. PCC (Pearson correlation coefficient): value can be −1–+1, where +1 indicates perfect correlation, −1 indicates perfect but negative correlation, 0 indicates the absence of a relationship. MOC (Mande's overlap coefficient): The value can be 0–1, where 1 indicates complete overlap and 0 indicates complete separation.[52–54] (c) Quantification of Alexa488-nucleic acid delivery to CPK4-pretreated HeLa cells using CPE4-LNP (200 μM, 200 μL) after incubation for 15 min in the presence of various endocytosis inhibitors. Fluorescence intensity was normalized to Alexa-488-nucleic acid delivery in the absence of inhibitors. (d) Quantification of cellular internalization efficiency of unmodified LNP (200 μM, 200 μL) after a 4 h incubation period in the presence of various endocytosis inhibitors. Error bars represent mean ± s.d. (representative dataset from n = 3 biologically independent samples).
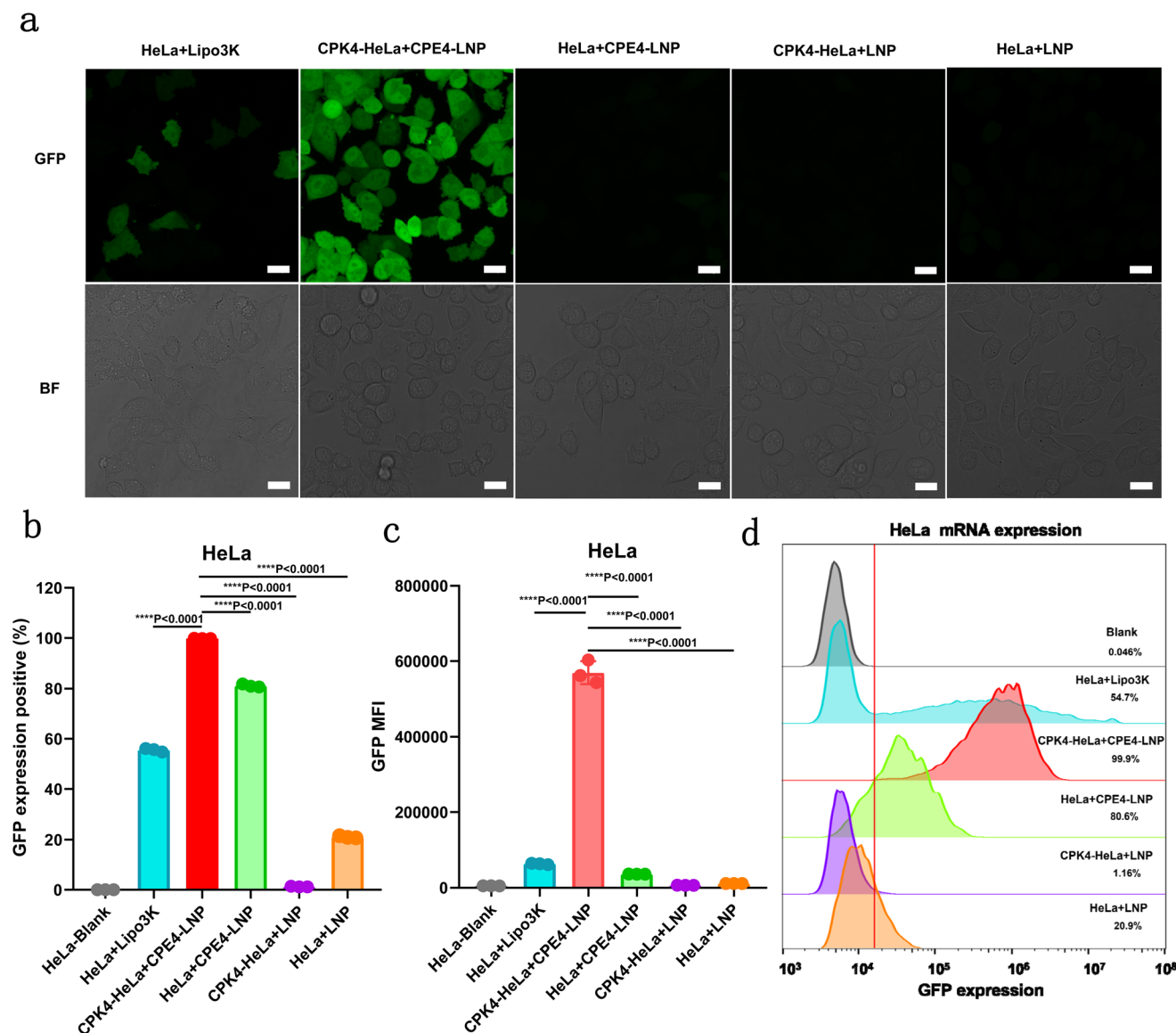
Fig. 5 Transfection efficiency of the coiled-coil system with HeLa cells. (a) Confocal images of the EGFP-mRNA transfection of LNPs. Lipo3K: lipofectamine 3000; GFP: green fluorescent protein; BF: bright field. The scale bar is 20 μm. (b) The quantification of EGFP-mRNA transfection efficiency of LNPs. (c and d) The GFP expression fluorescence intensity (GFP MFI) of LNPs. HeLa cells were first incubated with CPK4 (10 μM, 200 μL, 2 h), followed by incubation with EGFP-mRNA encapsulated LNPs (1 μg mL^{-1}, 2 h). Cells were then washed 3 times and cultured for another 18–24 h before confocal and flow cytometry measurements (representative dataset from n = 3 per group). Unpaired student t-test was used to determine the significance of the comparisons of data indicated in b, and c, (*P < 0.05; **P < 0.01; ***P < 0.001; ****P < 0.0001). In all panels, error bars represent mean $\pm$ s.d. (representative dataset from n = 3 biologically independent samples).

The mRNA transfection in T lymphocyte Jurkat cells was studied. Confocal imaging and flow cytometry data revealed that most Jurkat cells became GFP positive and GFP expression intensity (MFI) was the highest when the fusogenic coiled-coil peptides were used (Fig. S6a–d†). Again, transfection was significantly higher when compared to plain LNP or control groups missing one of the peptides. Interestingly, lipofectamine 3000 transfection of Jurkat cells was very inefficient. Overall, GFP expression levels in Jurkat were lower compared to HeLa cells, but still, the fusogenic coiled-coil LNP system induced a significant level of trans-

fection enhancement, which was >3-fold higher compared to LNP (Fig. S7d†).

To ensure that no cholesterol-PEG fusion peptides are released from the membrane, we performed the following experiment, see the protocol in Scheme S1.† We observed a specific CPE4 peak (rt = 5.31 min) in the groups of Pure CPE4 and CPE4-LNP formulation (Fig. S9a†). Meanwhile, the CPE4-Micelle solution after centrifugation also showed an identical CPE4 peak, which demonstrated that free CPE4 is able to pass through the 300 kDa cut-off membrane. However, no free CPE4 was detected after the separation from CPE4-LNP.

Therefore, we showed that the CPE4 did not dissociate from the CPE4-LNP. In another experiment, we studied the effect of free CPE4 on mRNA transfection (Fig. S9b†). For this, free CPE4 micelles were mixed with a batch of CPE4-LNPs and added to CPK4 pretreated HeLa cells. We showed that the presence of free CPE4 (10–40 mol% relative to CPE4 in CPE4-LNP) did not influence GFP expression.

In summary, LNP-mediated mRNA delivery using fusogenic coiled-coil peptides is an effective approach to obtaining high levels of protein expression in various cell lines and could act as a potent nonviral vector able to achieve efficient mRNA transfection of cells.

Cytotoxicity assay of LNPs

For successful nucleic acid-based therapies, it is important to keep a balance between transfection efficiency and cytotoxicity of the gene vector. Thus, the expression of GFP was studied as a function of the dose of LNPs carrying EGFP-mRNA, and the cell viability was determined in parallel. Near quantitative GFP expressing cells were obtained at a dose of 1 µg mL^{-1} EGFP-mRNA (Fig. S8a†). Next, cell viability after transfection was determined using the cell proliferation reagent WST-1. No significant toxicity was observed at all tested doses of EGFP-mRNA, and cell viability differences between plain LNP and coiled-coil modified LNP were not statistically significant. Interestingly, at higher doses the commercial reagent lipofectamine 3000 was shown to be more toxic (Fig. S8b†). Altogether, these results demonstrate that our coiled-coil gene delivery system achieves potent transfection efficiency without altering the cytotoxicity profile of LNPs.

Conclusions

Nonviral vectors can be used to encapsulate a wide variety of nucleic acid-based cargoes with a large range of molecular weights, including RNA (e.g. siRNA, mRNA, microRNA, ASO), DNA (e.g. plasmids), and genome editing tools (e.g. CRISPR/Cas, base editing, prime editing). The delivery of these cargoes using these vectors greatly facilitates precise and permanent correction of diseased genes.[2,55,56] Furthermore, multiple variants can be encapsulated and delivered using the same vector. To date, the design of novel nonviral vectors mainly focuses on establishing effective formulations capable of silencing, correcting, or introducing specific genes with minimal adverse effects.[2,57]

In this study, we showed that fusogenic coiled-coil peptides can induce efficient cellular internalization and potent transfection of nucleic acids in vitro. The introduction of 1 mol% of lipopeptide CPE4 to the LNP formulation did not alter physicochemical parameters such as size, zeta-potential, and mRNA encapsulation efficiency. However, CPE4 exerted a significantly enhanced internalization and transfection effect when target cells were pretreated with the complementary lipopeptide CPK4. Qualitative evaluation of transfection with confocal microscopy and quantitative analysis with flow cytometry revealed efficient nucleic acid uptake within 15 minutes of incubation when the fusogenic coiled-coil peptides were used. In contrast, plain LNP and all control groups were unable to deliver measurable amounts of nucleic acid within this timeframe. Coiled-coil mediated LNP transfection to cells is fast (within 2 hours of incubation) when compared to other cationic and lipid nanoparticles; these typically require longer incubation times (sometimes up to 72 h) to obtain significant transfection.[58,59] Furthermore we confirmed that the coiled-coil system is functional on various cell lines including CHO, NIH/3T3, and the hard-to-transfect Jurkat cells.

Gene delivery into cells using non-viral vectors often suffers from a poor ability to escape from the endosomal and/or lysosomal compartments. For siRNA, the endosomal escape was determined to be around 1–2%, making delivery very inefficient and thus lowering the potential therapeutic effect.[20] This is because endosomal escape is often spatio-temporally limited and only occurs in the brief stage of endo-lysosomal maturation.[20,40] Various approaches have been investigated to enhance endosomal escape efficiency, examples are the introduction of cell-penetrating peptides,[24,25] endosome disrupting peptides,[25,60] and photochemical internalization.[61,62] However, these approaches typically lack cell selectivity,[63] causing membrane destruction,[62] and resulting in cytotoxicity.[64,65] Using fusogenic coiled-coil peptides, we managed to circumvent endosomal entrapment and achieve direct cytosolic delivery of nucleic acid. This direct delivery was proven by performing uptake studies in the presence of common endocytosis inhibitors and quantifying the fraction of nucleic acid inside CPE4-LNP localized in lysosomes. Transfection of cells with EGFP-mRNA using fusogenic coiled-coil peptides resulted in an enhanced transfection performance as shown by the near-quantitative number of GFP positive cells and the high expression level of GFP in these cells as compared to plain LNP (up to a 63-fold increase in GFP expression). Furthermore, the control studies revealed that both coiled-coil peptides are required for efficient transfection, highlighting the importance of the coiled-coil interaction for the delivery of mRNA and concomitant protein expression. Our approach also outperformed the commercial reagent lipofectamine 3000 in all studies. Thus using fusogenic coiled-coil peptides lowers the amount of mRNA required to reach a desired expression level, which is also beneficial for cell viability. In this study, EGFP-mRNA was used, but any other nucleic acid could be delivered in a similar fashion.

The current approach requires the pretreatment of cells with CPK4, rendering it impractical for in vivo applications via systemic administration. Nevertheless, in vitro/ex vivo delivery and other in vivo delivery approaches other than i.v. injections, such as local/subcutaneous injections may be feasible. Since our approach has shown successful and enhanced genetic transfection on Jurkat cells, a potential application could be adoptive cell therapy.[66–68] Except for viral transduction, other attempts of lymphocyte transfection often apply electroporation and nucleofection to deliver exogenous genes into T cells,[69,70] but it requires specialized equipment, disrupts mem-

brane, produces cytokine, causes cytoplasmic content loss and cytotoxicity, and unable to penetrate membrane across cells consistently.[71,72] Coiled-coil mediated LNP delivery might also be applicable to the gene-editing field, such as CRISPR/Cas9 editing[73,74] and prime gene editing.[75] The highly efficient, transient, non-integrating Cas9 expression could greatly reduce the off-target effects, immune responses, and integration into the genome, which could be accomplished by our nonviral fusogenic coiled-coil delivery system.

In conclusion, fusogenic coiled-coil peptides can significantly enhance the delivery of nucleic acid to cells using LNPs. By circumventing the endosomal pathway, the genetic cargo is delivered to the cytosol of cells. For mRNA delivery, this resulted in an up to a 63-fold increase in protein expression as compared to unmodified LNP, opening new avenues for nucleic acid based therapies. Furthermore, we showed efficient transfection in various cell lines with substantial improvement as compared to the commercial transfection reagent lipofectamine 3000. Thus modification of LNPs with fusogenic coiled-coil peptides could serve as a promising strategy to enhance LNP efficacy to deliver nucleic acid based therapies *in vitro*, *ex vivo*, and potentially *in vivo*.

Data availability

The datasets supporting this article have been uploaded as part of the ESI.†

Author contributions

Y. Z. and A. K. conceived this research. Y. Z., M. S., R. P., X. Z., and Y. Z. performed the experiments. Y. Z., M. S., and R. P. analyzed the data with input from all authors. Y. Z., R. P., A. B., and A. K. wrote the manuscript with feedback from all authors. T. B. and T. H. S. provided support for flow cytometry and cryoEM. A. K. managed the project.

Conflicts of interest

The authors declare no competing interests.

Acknowledgements

References

1 A. Akinc, M. A. Maier, M. Manoharan, K. Fitzgerald, M. Jayaraman, S. Barros, S. Ansell, X. Du, M. J. Hope, T. D. Madden, B. L. Mui, S. C. Semple, Y. K. Tam, M. Ciufolini, D. Witzigmann, J. A. Kulkarni, R. van der Meel and P. R. Cullis, *Nat. Nanotechnol.*, 2019, **14**, 1084–1087.

2 Y. Dong, K. T. Love, J. R. Dorkin, S. Sirirungruang, Y. Zhang, D. Chen, R. L. Bogorad, H. Yin, Y. Chen, A. J. Vegas, C. A. Alabi, G. Sahay, K. T. Olejnik, W. Wang, A. Schroeder, A. K. Lytton-Jean, D. J. Siegwart, A. Akinc, C. Barnes, S. A. Barros, M. Carioto, K. Fitzgerald, J. Hettinger, V. Kumar, T. I. Novobrantseva, J. Qin, W. Querbes, V. Koteliansky, R. Langer and D. G. Anderson, *Proc. Natl. Acad. Sci. U. S. A.*, 2014, **111**, 3955–3960.

3 S. Guan and J. Rosenecker, *Gene Ther.*, 2017, **24**, 133–143.

4 L. Naldini, *Nature*, 2015, **526**, 351–360.

5 N. Somia and I. M. Verma, *Nat. Rev. Genet.*, 2000, **1**, 91–99.

6 C. Li and R. J. Samulski, *Nat. Rev. Genet.*, 2020, **21**, 255–272.

7 D. A. Kuzmin, M. V. Shutova, N. R. Johnston, O. P. Smith, V. V. Fedorin, Y. S. Kukushkin, J. C. M. van der Loo and E. C. Johnstone, *Nat. Rev. Drug Discovery*, 2021, **20**, 173–174.

8 C. E. Dunbar, K. A. High, J. K. Joung, D. B. Kohn, K. Ozawa and M. Sadelain, *Science*, 2018, **359**, eaan4672.

9 C. E. Thomas, A. Ehrhardt and M. A. Kay, *Nat. Rev. Genet.*, 2003, **4**, 346–358.

10 N. Bessis, F. J. GarciaCozar and M. C. Boissier, *Gene Ther.*, 2004, **11**(Suppl 1), S10–S17.

11 H. Yin, R. L. Kanasty, A. A. Eltoukhy, A. J. Vegas, J. R. Dorkin and D. G. Anderson, *Nat. Rev. Genet.*, 2014, **15**, 541–555.

12 S. Sabnis, E. S. Kumarasinghe, T. Salerno, C. Mihai, T. Ketova, J. J. Senn, A. Lynn, A. Bulychev, I. McFadyen, J. Chan, O. Almarsson, M. G. Stanton and K. E. Benenato, *Mol. Ther.*, 2018, **26**, 1509–1519.

13 D. Witzigmann, J. A. Kulkarni, J. Leung, S. Chen, P. R. Cullis and R. van der Meel, *Adv. Drug Delivery Rev.*, 2020, **159**, 344–363.

14 Y. Zhang, C. Sun, C. Wang, K. E. Jankovic and Y. Dong, *Chem. Rev.*, 2021, **121**, 12181–12277.

15 S. Yonezawa, H. Koide and T. Asai, *Adv. Drug Delivery Rev.*, 2020, **154–155**, 64–78.

16 Y. Zeng, O. Escalona-Rayo, R. Knol, A. Kros and B. Slütter, *Biomater. Sci.*, 2023, **11**, 964–974.

17 P. S. Kowalski, A. Rudra, L. Miao and D. G. Anderson, *Mol. Ther.*, 2019, **27**, 710–728.

18 A. Akinc, W. Querbes, S. De, J. Qin, M. Frank-Kamenetsky, K. N. Jayaprakash, M. Jayaraman, K. G. Rajeev, W. L. Cantley, J. R. Dorkin, J. S. Butler, L. Qin, T. Racie, A. Sprague, E. Fava, A. Zeigerer, M. J. Hope, M. Zerial, D. W. Sah, K. Fitzgerald, M. A. Tracy, M. Manoharan, V. Koteliansky, A. Fougerolles and M. A. Maier, *Mol. Ther.*, 2010, **18**, 1357–1364.

19 A. Wittrup, A. Ai, X. Liu, P. Hamar, R. Trifonova, K. Charisse, M. Manoharan, T. Kirchhausen and J. Lieberman, *Nat. Biotechnol.*, 2015, **33**, 870–876.

20 J. Gilleron, W. Querbes, A. Zeigerer, A. Borodovsky, G. Marsico, U. Schubert, K. Manygoats, S. Seifert,

C. Andree, M. Stoter, H. Epstein-Barash, L. Zhang, V. Koteliansky, K. Fitzgerald, E. Fava, M. Bickle, Y. Kalaidzidis, A. Akinc, M. Maier and M. Zerial, *Nat. Biotechnol.*, 2013, **31**, 638–646.

21 P. Paramasivam, C. Franke, M. Stoter, A. Hoijer, S. Bartesaghi, A. Sabirsh, L. Lindfors, M. Y. Arteta, A. Dahlen, A. Bak, S. Andersson, Y. Kalaidzidis, M. Bickle and M. Zerial, *J. Cell Biol.*, 2022, **221**, e202110137.

22 I. M. S. Degors, C. Wang, Z. U. Rehman and I. S. Zuhorn, *Acc. Chem. Res.*, 2019, **52**, 1750–1760.

23 J. Zhu, M. Qiao, Q. Wang, Y. Ye, S. Ba, J. Ma, H. Hu, X. Zhao and D. Chen, *Biomaterials*, 2018, **162**, 47–59.

24 T. Endoh and T. Ohtsuki, *Adv. Drug Delivery Rev.*, 2009, **61**, 704–709.

25 Y. H. Wang, Y. W. Hou and H. J. Lee, *J. Biochem. Biophys. Methods*, 2007, **70**, 579–586.

26 H. D. Do, B. M. Couillaud, B. T. Doan, Y. Corvis and N. Mignet, *Adv. Drug Delivery Rev.*, 2019, **138**, 3–17.

27 Y. A. Chen and R. H. Scheller, *Nat. Rev. Mol. Cell Biol.*, 2001, **2**, 98–106.

28 R. Jahn and R. H. Scheller, *Nat. Rev. Mol. Cell Biol.*, 2006, **7**, 631–643.

29 J. Yang, A. Bahreman, G. Daudey, J. Bussmann, R. C. Olsthoorn and A. Kros, *ACS Cent. Sci.*, 2016, **2**, 621–630.

30 J. Yang, Y. Shimada, R. C. Olsthoorn, B. E. Snaar-Jagalska, H. P. Spaink and A. Kros, *ACS Nano*, 2016, **10**, 7428–7435.

31 L. Kong, S. H. Askes, S. Bonnet, A. Kros and F. Campbell, *Angew. Chem., Int. Ed.*, 2016, **55**, 1396–1400.

32 Y. Zeng, M. Shen, A. Singhal, G. J. A. Sevink, N. Crone, A. L. Boyle and A. Kros, *Small*, 2023, 2301133.

33 H. R. Zope, F. Versluis, A. Ordas, J. Voskuhl, H. P. Spaink and A. Kros, *Angew. Chem., Int. Ed.*, 2013, **52**, 14247–14251.

34 F. Versluis, J. Voskuhl, B. van Kolck, H. Zope, M. Bremmer, T. Albregtse and A. Kros, *J. Am. Chem. Soc.*, 2013, **135**, 8057–8062.

35 A. O. Tezgel, G. Gonzalez-Perez, J. C. Telfer, B. A. Osborne, L. M. Minter and G. N. Tew, *Mol. Ther.*, 2013, **21**, 201–209.

36 C. J. McKinlay, N. L. Benner, O. A. Haabeth, R. M. Waymouth and P. A. Wender, *Proc. Natl. Acad. Sci. U. S. A.*, 2018, **115**, E5859–E5866.

37 Y. Xie, N. H. Kim, V. Nadithe, D. Schalk, A. Thakur, A. Kilic, L. G. Lum, D. J. P. Bassett and O. M. Merkel, *J. Controlled Release*, 2016, **229**, 120–129.

38 Q. Ding, X. Si, D. Liu, J. Peng, H. Tang, W. Sun, M. Rui, Q. Chen, L. Wu and Y. Xu, *J. Controlled Release*, 2015, **207**, 86–92.

39 I. M. S. Degors, C. Wang, Z. U. Rehman and I. S. Zuhorn, *Acc. Chem. Res.*, 2019, **52**, 1750–1760.

40 S. Patel, N. Ashwanikumar, E. Robinson, A. DuRoss, C. Sun, K. E. Murphy-Benenato, C. Mihai, O. Almarsson and G. Sahay, *Nano Lett.*, 2017, **17**, 5711–5718.

41 A. Arcaro and M. P. Wymann, *Biochem. J.*, 1993, **296**, 297–301.

42 W. Tao, X. Mao, J. P. Davide, B. Ng, M. Cai, P. A. Burke, A. B. Sachs and L. Sepp-Lorenzino, *Mol. Ther.*, 2011, **19**, 567–575.

43 D. Vercauteren, M. Piest, L. J. van der Aa, M. Al Soraj, A. T. Jones, J. F. Engbersen, S. C. De Smedt and K. Braeckmans, *Biomaterials*, 2011, **32**, 3072–3084.

44 L. von Kleist, W. Stahlschmidt, H. Bulut, K. Gromova, D. Puchkov, M. J. Robertson, K. A. MacGregor, N. Tomilin, A. Pechstein, N. Chau, M. Chircop, J. Sakoff, J. P. von Kries, W. Saenger, H. G. Krausslich, O. Shupliakov, P. J. Robinson, A. McCluskey and V. Haucke, *Cell*, 2011, **146**, 471–484.

45 E. Macia, M. Ehrlich, R. Massol, E. Boucrot, C. Brunner and T. Kirchhausen, *Dev. Cell*, 2006, **10**, 839–850.

46 G. Preta, J. G. Cronin and I. M. Sheldon, *Cell Commun. Signaling*, 2015, **13**, 24.

47 D. Vercauteren, R. E. Vandenbroucke, A. T. Jones, J. Rejman, J. Demeester, S. C. De Smedt, N. N. Sanders and K. Braeckmans, *Mol. Ther.*, 2010, **18**, 561–569.

48 J. Rejman, A. Bragonzi and M. Conese, *Mol. Ther.*, 2005, **12**, 468–474.

49 S. K. Rodal, G. Skretting, Ø. Garred, F. Vilhardt, B. van Deurs and K. Sandvig, *Mol. Biol. Cell*, 1999, **10**, 961–974.

50 S. Novakowski, K. Jiang, G. Prakash and C. Kastrup, *Sci. Rep.*, 2019, **9**, 552.

51 G. Sahay, W. Querbes, C. Alabi, A. Eltoukhy, S. Sarkar, C. Zurenko, E. Karagiannis, K. Love, D. Chen, R. Zoncu, Y. Buganim, A. Schroeder, R. Langer and D. G. Anderson, *Nat. Biotechnol.*, 2013, **31**, 653–658.

52 J. Adler and I. Parmryd, *Cytometry, Part A*, 2010, **77A**, 733–742.

53 J. S. Aaron, A. B. Taylor and T.-L. Chew, *J. Cell Sci.*, 2018, **131**, jcs211847.

54 K. W. Dunn, M. M. Kamocka and J. H. McDonald, *Am. J. Physiol.: Cell Physiol.*, 2011, **300**, C723–C742.

55 K. A. Hajj and K. A. Whitehead, *Nat. Rev. Mater.*, 2017, **2**, 17056.

56 J. B. Miller, S. Zhang, P. Kos, H. Xiong, K. Zhou, S. S. Perelman, H. Zhu and D. J. Siegwart, *Angew. Chem., Int. Ed.*, 2017, **56**, 1059–1063.

57 M. Krohn-Grimberghe, M. J. Mitchell, M. J. Schloss, O. F. Khan, G. Courties, P. P. G. Guimaraes, D. Rohde, S. Cremer, P. S. Kowalski, Y. Sun, M. Tan, J. Webster, K. Wang, Y. Iwamoto, S. P. Schmidt, G. R. Wojtkiewicz, R. Nayar, V. Frodermann, M. Hulsmans, A. Chung, F. F. Hoyer, F. K. Swirski, R. Langer, D. G. Anderson and M. Nahrendorf, *Nat. Biomed. Eng.*, 2020, **4**, 1076–1089.

58 C. D. Sago, M. P. Lokugamage, K. Paunovska, D. A. Vanover, C. M. Monaco, N. N. Shah, M. Gamboa Castro, S. E. Anderson, T. G. Rudoltz, G. N. Lando, P. Munnilal Tiwari, J. L. Kirschman, N. Willett, Y. C. Jang, P. J. Santangelo, A. V. Bryksin and J. E. Dahlman, *Proc. Natl. Acad. Sci. U. S. A.*, 2018, **115**, E9944–E9952.

59 R. L. Ball, K. A. Hajj, J. Vizelman, P. Bajaj and K. A. Whitehead, *Nano Lett.*, 2018, **18**, 3814–3822.

60 S. M. Van Rossenberg, K. M. Sliedregt-Bol, N. J. Meeuwenoord, T. J. Van Berkel, J. H. Van Boom, G. A. Van Der Marel and E. A. Biessen, *J. Biol. Chem.*, 2002, **277**, 45803–45810.

61 K. G. de Bruin, C. Fella, M. Ogris, E. Wagner, N. Ruthardt and C. Brauchle, *J. Controlled Release*, 2008, **130**, 175–182.

62 P. K. Selbo, A. Weyergang, A. Hogset, O. J. Norum, M. B. Berstad, M. Vikdal and K. Berg, *J. Controlled Release*, 2010, **148**, 2–12.

63 W. Tai and X. Gao, *Adv. Drug Delivery Rev.*, 2017, **110–111**, 157–168.

64 K. Saar, M. Lindgren, M. Hansen, E. Eiriksdottir, Y. Jiang, K. Rosenthal-Aizman, M. Sassian and U. Langel, *Anal. Biochem.*, 2005, **345**, 55–65.

65 T. F. Martens, K. Remaut, J. Demeester, S. C. De Smedt and K. Braeckmans, *Nano Today*, 2014, **9**, 344–364.

66 U. Sahin, K. Kariko and O. Tureci, *Nat. Rev. Drug Discovery*, 2014, **13**, 759–780.

67 J. B. Foster, D. M. Barrett and K. Kariko, *Mol. Ther.*, 2019, **27**, 747–756.

68 S. A. Rosenberg and N. P. Restifo, *Science*, 2015, **348**, 62–68.

69 T. DiTommaso, J. M. Cole, L. Cassereau, J. A. Bugge, J. L. S. Hanson, D. T. Bridgen, B. D. Stokes, S. M. Loughhead, B. A. Beutel, J. B. Gilbert, K. Nussbaum, A. Sorrentino, J. Toggweiler, T. Schmidt, G. Gyuelveszi, H. Bernstein and A. Sharei, *Proc. Natl. Acad. Sci. U. S. A.*, 2018, **115**, E10907–E10914.

70 T. L. Roth, C. Puig-Saus, R. Yu, E. Shifrut, J. Carnevale, P. J. Li, J. Hiatt, J. Saco, P. Krystofinski, H. Li, V. Tobin, D. N. Nguyen, M. R. Lee, A. L. Putnam, A. L. Ferris, J. W. Chen, J. N. Schickel, L. Pellerin, D. Carmody, G. Alkorta-Aranburu, D. Del Gaudio, H. Matsumoto, M. Morell, Y. Mao, M. Cho, R. M. Quadros, C. B. Gurumurthy, B. Smith, M. Haugwitz, S. H. Hughes, J. S. Weissman, K. Schumann, J. H. Esensten, A. P. May, A. Ashworth, G. M. Kupfer, S. A. W. Greeley, R. Bacchetta, E. Meffre, M. G. Roncarolo, N. Romberg, K. C. Herold, A. Ribas, M. D. Leonetti and A. Marson, *Nature*, 2018, **559**, 405–409.

71 Y. Zhao, Z. Zheng, C. J. Cohen, L. Gattinoni, D. C. Palmer, N. P. Restifo, S. A. Rosenberg and R. A. Morgan, *Mol. Ther.*, 2006, **13**, 151–159.

72 X. Wang and I. Riviere, *Mol. Ther.–Oncolytics*, 2016, **3**, 16015.

73 J. D. Finn, A. R. Smith, M. C. Patel, L. Shaw, M. R. Youniss, J. van Heteren, T. Dirstine, C. Ciullo, R. Lescarbeau, J. Seitzer, R. R. Shah, A. Shah, D. Ling, J. Growe, M. Pink, E. Rohde, K. M. Wood, W. E. Salomon, W. F. Harrington, C. Dombrowski, W. R. Strapps, Y. Chang and D. V. Morrissey, *Cell Rep.*, 2018, **22**, 2227–2235.

74 J. Liu, J. Chang, Y. Jiang, X. Meng, T. Sun, L. Mao, Q. Xu and M. Wang, *Adv. Mater.*, 2019, **31**, 1902575.

75 A. V. Anzalone, P. B. Randolph, J. R. Davis, A. A. Sousa, L. W. Koblan, J. M. Levy, P. J. Chen, C. Wilson, G. A. Newby, A. Raguram and D. R. Liu, *Nature*, 2019, **576**, 149–157.